Electronic Supplementary Material (ESI) for Journal of Materials Chemistry C.

Supporting Information

Mobility calculation

The FET mobility values were calculated using the following equation, $\mu = [dI_{ds}/dV_{bg}] \times [L/(WC_iV_{ds})]$, where W is the channel width, L is the channel length and C_i (1.5×10^{-4} F/m^2) is the capacitance between the channel and the back gate per unit area ($C_i = \varepsilon\times\varepsilon_r/d$; $\varepsilon_o = 8.85\times10^{-12}$ F·m^{-1}, $\varepsilon_r = 3.9$; d = 230 nm) (Adv. Mater. 2011, **23**, 4178). The device parameters L, C_i were the same as used earlier (Scientific Reports. 2018, **8**, 8586).

Temperature dependent electrical transport properties

Temperature dependent electrical transport behavior is understood based on Richardson's equation (*Nano Lett*. 2013, **13**, 3106-3110).

$$I_{ds} = AA^{*}T^{3/2}e^{\left[-\frac{q}{kBT}\left(\Phi B - \frac{V_{ds}}{n}\right)\right]}$$

where A is contact area of the junction, A* is the Richardson constant, q is magnitude of electron charge, Φ_B is the Schottky barrier height, k_B is Boltzmann constant, n is ideality factor, V_{ds} is drain-source voltage and T is the temperature.The intercept observed in Fig. S3(d) is denoted S_o and used to calculate Schottky barrier height using the equation,

$$S_0 = -\frac{q\Phi B}{1000K_B}$$

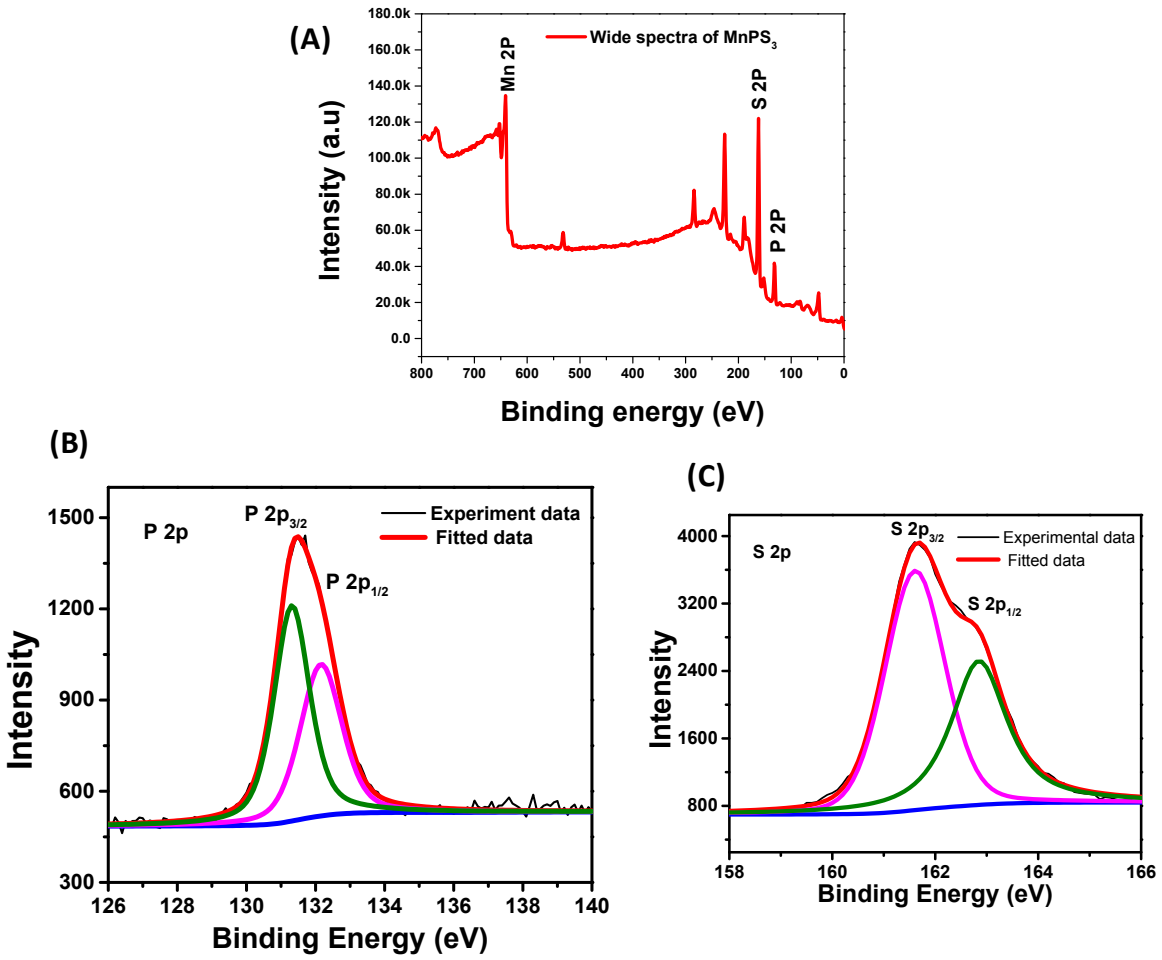

Fig. S1. (a) XPS survey spectrum of bulk $MnPS_3$. High resolution spectral regions of (b) P 2p and (c) S 2p levels are shown.

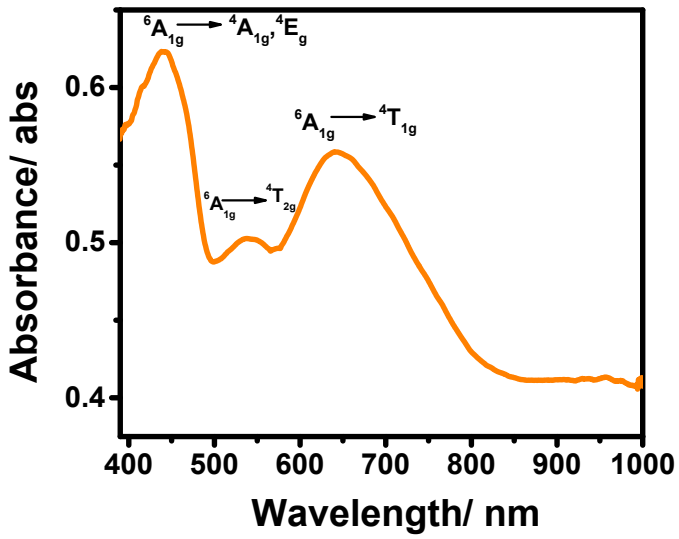

Fig. S2. Absorbance vs wavelength for solid $MnPS_3$.

Three absorption bands corresponding to electronic transitions into the 3d-shell of Mn^{2+} have been observed and is similar to the reported spectrum (*Phy. Rev. B*, 1991, **44**, 11060). The transitions are assigned to, $^6A_{1g} \rightarrow {}^4T_{1g}$ at 640 nm, $^6A_{1g} \rightarrow {}^4T_{2g}$ at 540 nm and $^6A_{1g} \rightarrow {}^4A_{1g}$, ^4E_g at 440 nm.

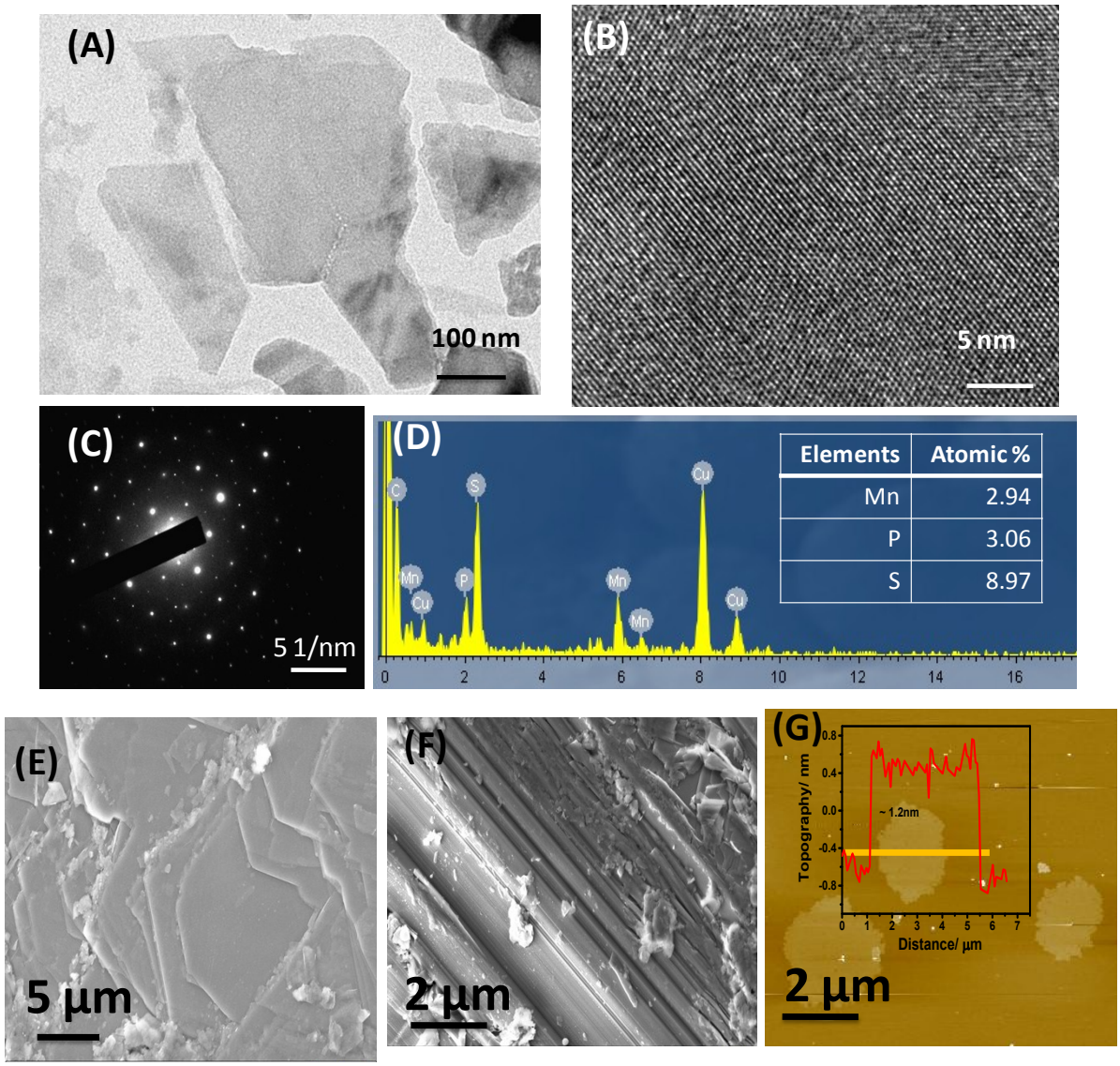

Fig. S3(a). TEM images of liquid exfoliated $MnPS_3$. (b) HRTEM images of few layer of $MnPS_3$, (c) corresponding SAED pattern. (d) EDS mapping showing the elemental ratio of Mn, P and S to be ~ 1:1:3 (e) SEM of bulk $MnPS_3$ (f) edge of a flake showing layered nature and (g) AFM of single layer $MnPS_3$.

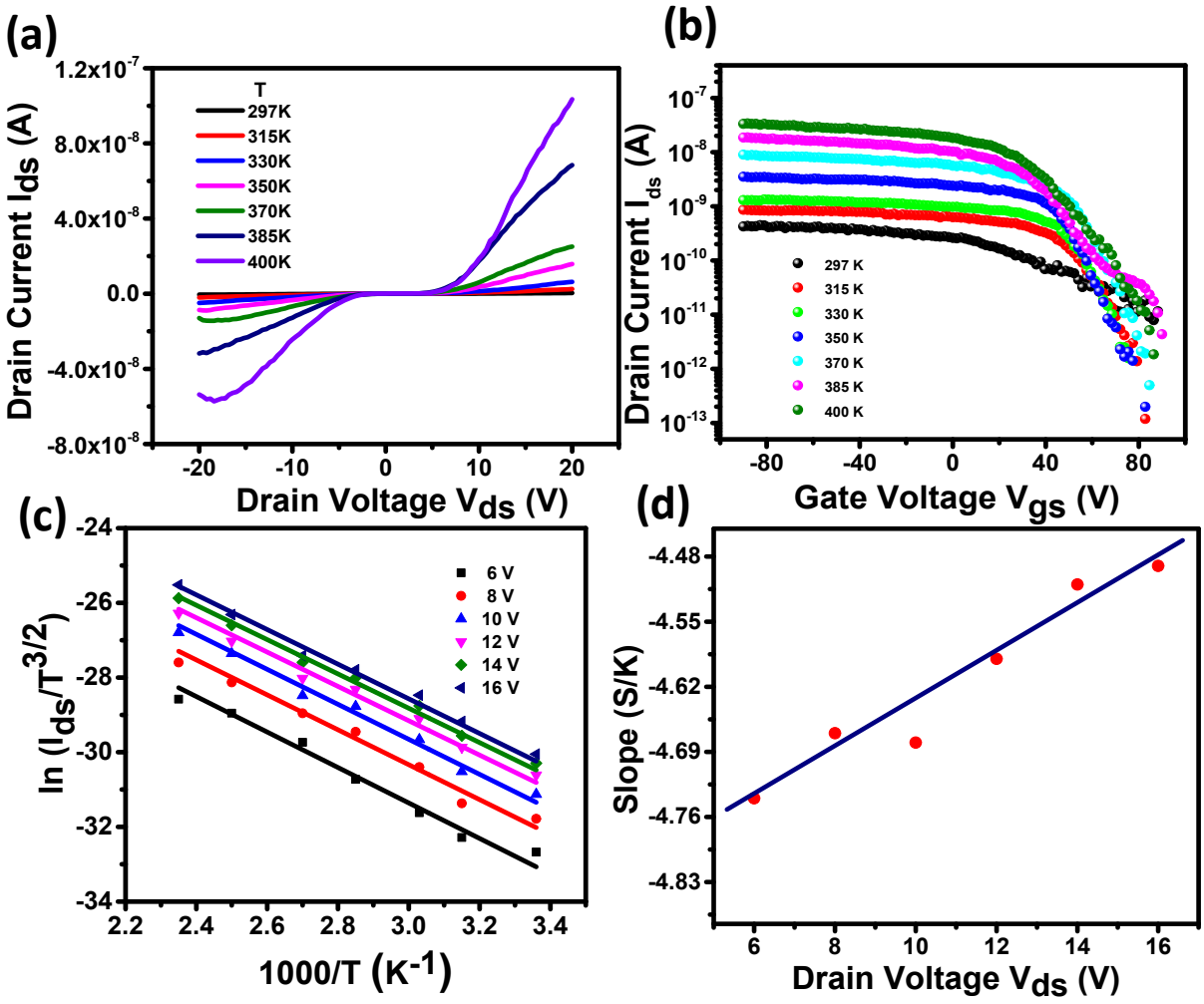

Fig. S4. (a) Temperature dependence of I_{ds} as a function of V_{ds} at zero gate bias. (b) Transfer characteristics I_{ds} vs V_{gs} at V_{ds} = 8V. (c) Arrehenius plots of $\ln(I_{ds}/T^{3/2})$ vs 1000/T derived from the data given in Fig. S4(a). (d) Slope extracted from Arrehenius plots as a function of V_{ds}.

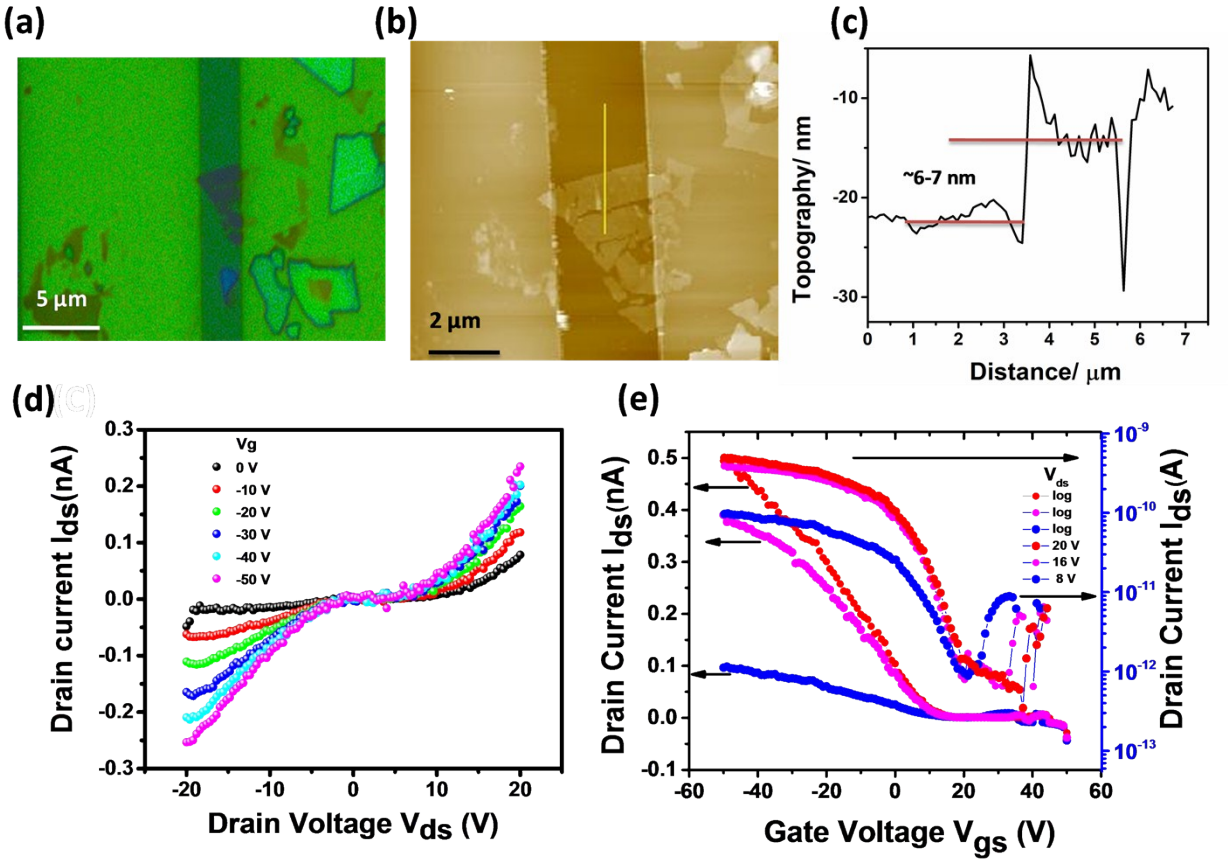

Fig. S5. (a) Optical micrograph of a typical $MnPS_3$ device. (b) AFM image of 6-7 nm $MnPS_3$ flake on Si/SiO_2 with ITO/Au contact pads and (c) height profile (d) I_{ds} versus V_{ds} characteristics and (e) corresponding transfer characteristics.

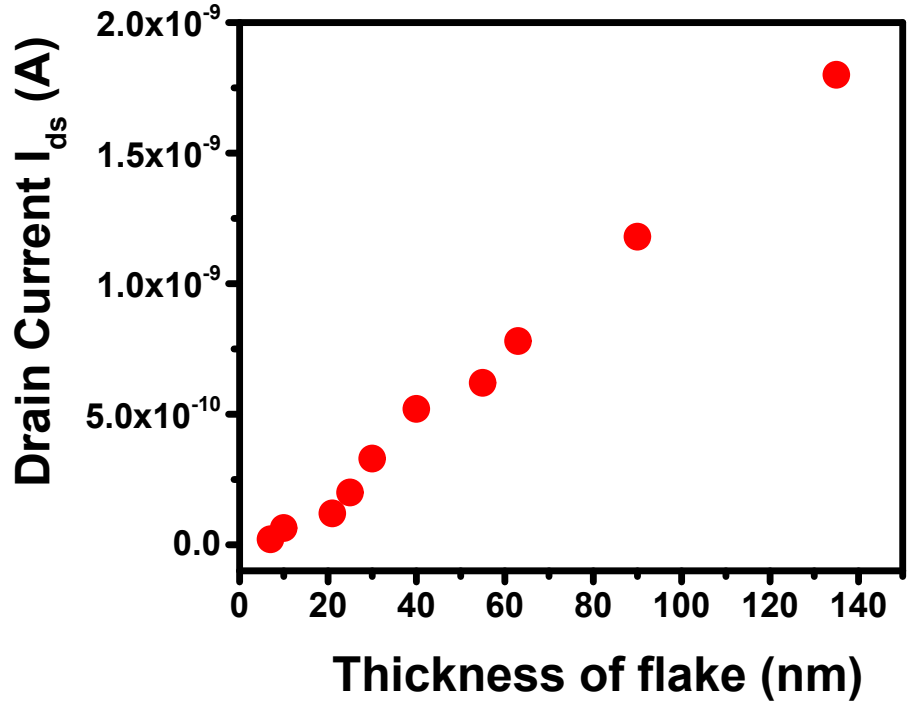

Fig. S6. Drain current variation with thickness of $MnPS_3$.

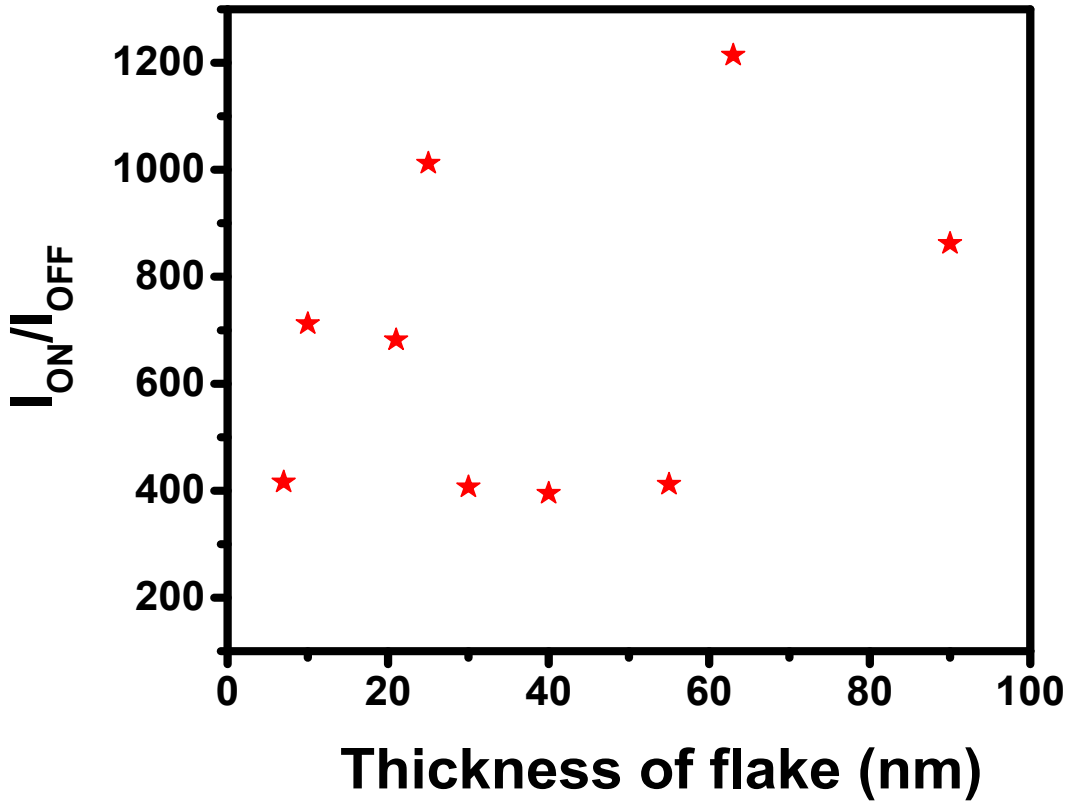

Fig. S7. Current on-off ratio with thickness of $MnPS_3$ device.

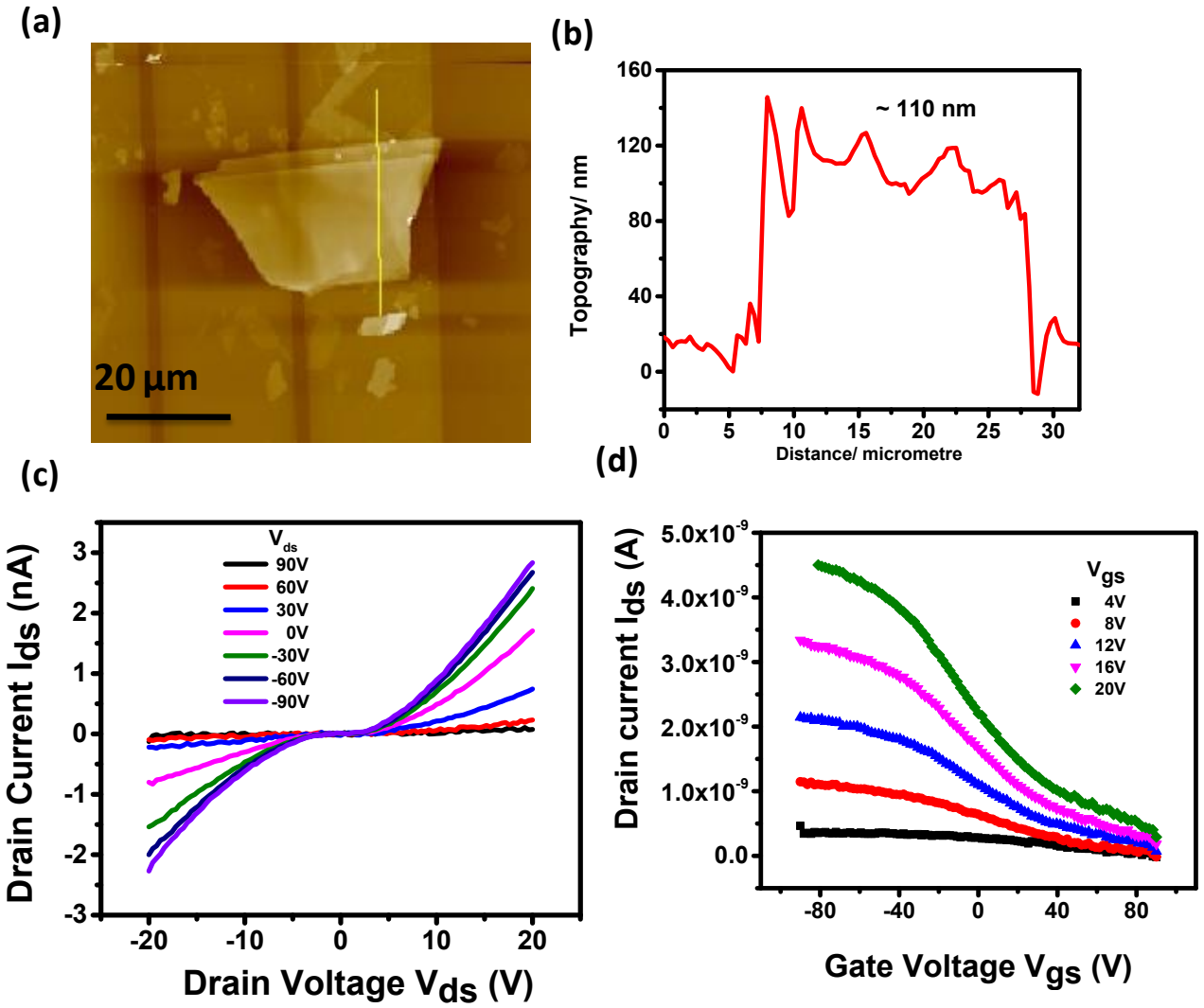

Fig. S8. (a) and (b) AFM image of 110 nm $MnPS_3$ device along with height profile (c) FET data, output characteristics (I_{ds}-V_{ds}) and (d) transfer characteristics, (I_{ds}-V_{bg}) behaviour.

Photo device performance

Photoresponsivity (Rp), photogain (G), and detectivity (D*) are calculated using following equation. Photoresponsitivity is defined as, $$R_p = \frac{I_p}{AP_{light}}$$

where Ip is the photocurrent (Ip = I_{light}– I_{dark}) and P_{light} is the power of incident illumination and A is effective area of device.

The photogain is defined as, $$G = \frac{R_p \times h \times C}{q\lambda}$$

where h is Plank's constant, c is speed of light, q is electronic charge and λ is wavelength of light.

Specific detectivity is defined as,

$$D^* = \frac{R_p\sqrt{A}}{\sqrt{2qI_d}}$$

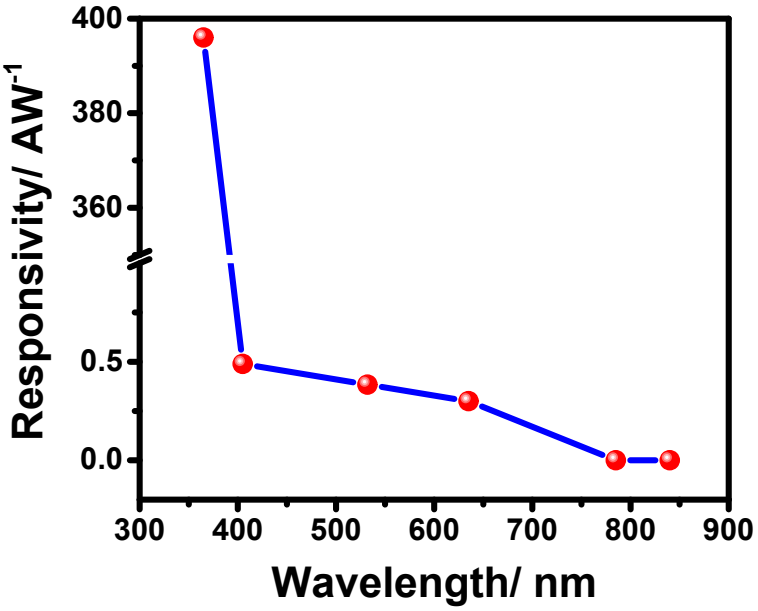

Fig. S9. Photoresposivity vs wavelength for multilayer $MnPS_3$.

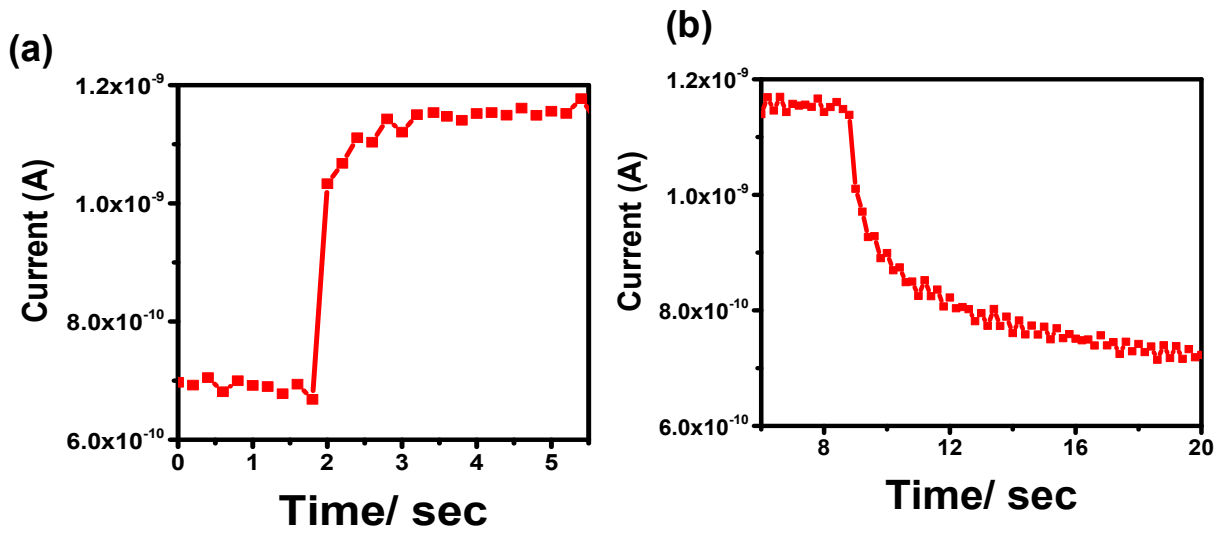

Fig. S10. Photocurrent response of the device (a) rise and (b) decay profiles.

Table S1. Comparison of photoresponse of $MnPS_3$ with other reported 2D materials.

Material	Responsivity AW^{-1}	Response time ms	Detectivity Jones	Reference
MoS_2 (Mech. exfol. single layer)	7.5×10^{-3}	50	-	S1
MoS_2 (Mech. exfol. single layer)	880	600	-	S2
MoS_2 (Mech. exfol. multilayer)	0.12	-	10^{11}	S3
MoS_2 (CVD grown single layer)	1.1×10^{-3}	$> 10^3$	-	S4
MoS_2 (CVD grown few - layer)	0.57	7.0×10^{-2}	10^{10}	S5
$MoSe_2$ (Mech. exfol. few-layer)	97.1	15	-	S6

$MoSe_2$ (CVD grown single layer)	2.15×10^{-4}	25	-	S7
$MoSe_2$ (CVD grown multi-layer)	93.7	400	-	S8
$MoTe_2$ (Mech. exfol. few - layer)	2560	-	-	S9
WS_2 (CVD grown few - layer)	9.2×10^{-5}	5.3	-	S10
WS_2 (PLD grown multi-layer)	0.70	9.9×10^{3}	2.7×10^{9}	S11
WSe_2 (Mech. exfol. three layers)	7	1×10^{-2}	-	S12
WSe_2 (CVD grown monolayer)	1.1	$> 10^{3}$	-	S13
HfS_2 (Mech. exfol. few - layer)	890	38	1.3×10^{10}	S14
$ReSe_2$ (Mech. exfol. single layer)	95	68	-	S15
ReS_2 (Mech. exfol. few - layer)	$>10^{3}$	98	-	S16
ReS_2 (CVD grown few - layer)	16.14	$>10^{5}$	-	S17
ReS_2 (Mech. exfol. few - layer)	8.86×10^{4}	$>10^{5}$	1.18×10^{12}	S18
GaS (Mech. exfol. few - layer)	64.43	13	-	S19
GaSe (Mech. Exfol few - layer)	2.8	20	-	S20
GaSe (Mech. exfol. multi-layer)	5×10^{3}	10	-	S21

GaTe (Mech. exfol. multi-layer)	$>10^4$	6	-	S22
GaTe (CVD grown multi-layer)	0.03	54	-	S23
InSe (Mech. exfol. few - layer)	157	50	1.07×10^{11}	S24
In_2Se_3 (Mech. exfol. ten layers)	3.95×10^2	18	2.26×10^{12}	S25
SnS_2 (Mech. exfol. few - layer)	100	44	-	S26
SnS_2 (CVD grown multi-layer)	100	22	-	S27
$SnSe_2$ (Mech. exfol. bilayer)	0.5	2.1	-	S28
GeS (Mech. exfol. multi-layer)	655	7	2.35×10^{13}	S29
TiS_3 (Mech. exfol. few layer)	2.91×10^3	4	-	S30
BP (Mech. exfol. few -layer)	4.8×10^{-3}	1	-	S31
BP (Mech. exfol. multi-layer)	2×10^{-2}	-	-	S32
$NiPS_3$ (Mech. exfol. few layer)	0.126	3.2	1.22×10^{12}	35 (manuscript)
$FePS_3$ (Mech. exfol. few - layer)	0.171	105	-	36 (manuscript)
$MnPS_3$ (Mech. exfol. multi-layer – 50 layers)	**288**	**340**	**6.48×10^{11}**	**Current work**

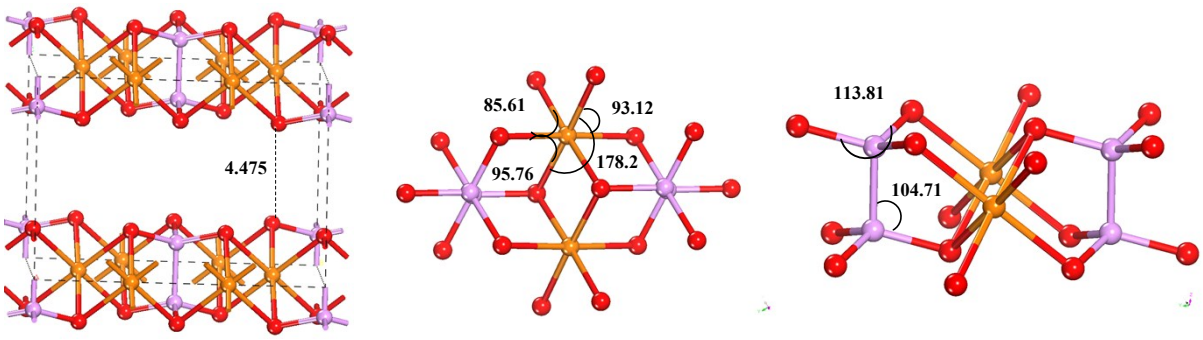

Fig. S11. Geometric parameters used to measure distortion angle. The red, pink, orange as represents sulphur, phosphorus, and manganese atoms.

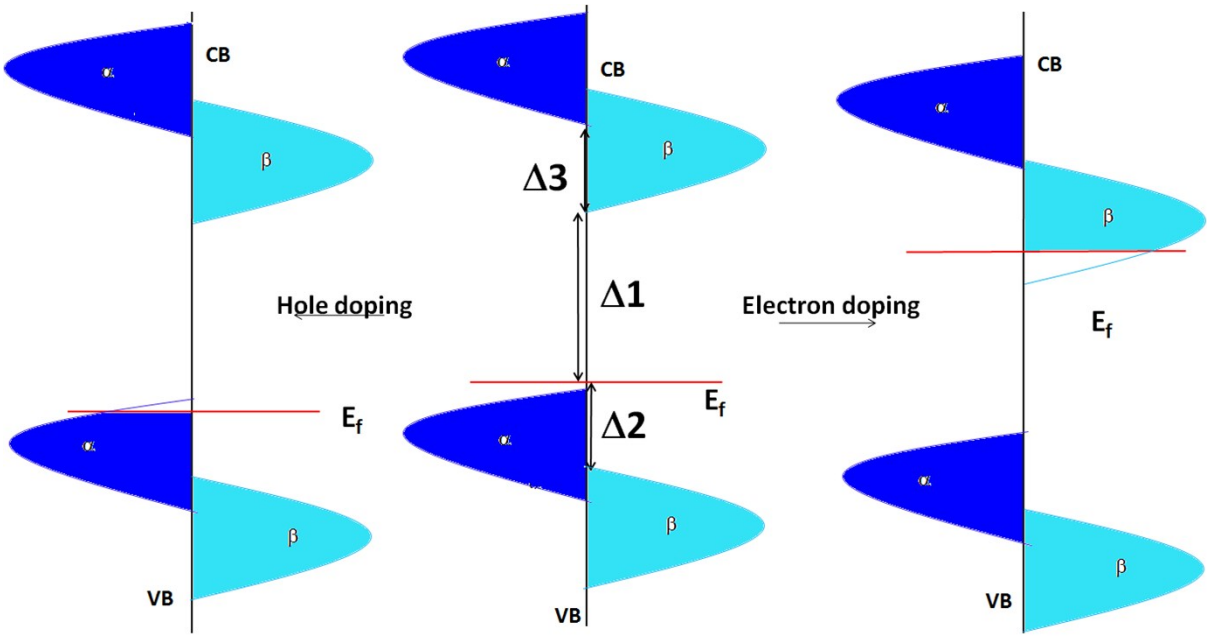

Fig. S12. Schematic diagram depicting the band structure for different spin polarized BMS material upon electron/hole doping.

Table S2: S-Mn-S bond angles for bulk $MnPS_3$, electron doped- and hole doped- bulk $MnPS_3$.

S.No	S-Mn-S		
	Bulk $MnPS_3$	Hole doped $MnPS_3$	Electron doped $MnPS_3$
1	85.549	96.257	87.193
2	95.547	84.147	94.493
3	85.636	84.227	91.206
4	93.112	95.378	87.193
5	85.614	96.74	87.153
6	93.215	94.44	87.193
7	95.757	84.413	91.206
8	85.636	84.413	94.493
9	93.112	96.257	87.205
10	85.549	84.147	94.265
11	95.757	95.378	91.38
12	85.614	94.237	87.204

Table S3.Geometric parameters obtained using DFT for layered neutral $MnPS_3$. Experimentally observed crystal structure parameters are shown for comparison.

Material	Bond length (Å)			Bond angles (°)				Lattice Parameters
	P-S	Mn-S	P-P	Mn-S-Mn	Mn-S-P	S-P-S	S-P-P	
$MnPS_3$ neutral (Exp.)	2.0296 2.0342	2.6343 2.6215 2.6193	2.1874	85.78	103.41	113.41 113.31	105.28	a,b,c = 6.077, 10.524, 6.796 α,β,γ = 90, 107.35, 90
$MnPS_3$- neutral (Theory)	2.0438 2.0444	2.6144 2.6148 2.6157	2.2080	84.45	103.62	113.81 113.84	104.57 104.71	a,b,c= 6.07817, 10.53306, 10.833341 α,β,γ =90, 138.32, 90

Table S4. Geometric parameters obtained using DFT for $MnPS_3$ with hole and electron doping.

Material	Bond length (Å)			Bond angles (°)				Lattice Parameters
	P-S	Mn-S	P-P	Mn-S-Mn	Mn-S-P	S-P-S	S-P-P	
$MnPS_3$ 0.1electron /atom	2.0570 2.0576	2.6304 2.6269 2.6233	2.2148	85.51	105.17	114.647 114.767	103.55 103.56	6.1828, 10.7054, 9.7856 α,β,γ =90, 102.16,90
$MnPS_3$ 0.1hole /atom	2.0371 2.0412	2.5011 2.5012 2.5094	2.1866	84.62	102.64	114.77 114.65	103.52 104.15	6.1828, 10.7054, 9.78556 α,β,γ =90, 102.16, 90
$MnPS_3$ neutral (Theory)	2.0438 2.0444	2.6144 2.6148 2.6157	2.2080	84.45	103.62	113.81 113.84	104.57 104.71	a,b,c= 6.07817, 10.53306, 10.833341 α,β,γ =90, 138.32, 90

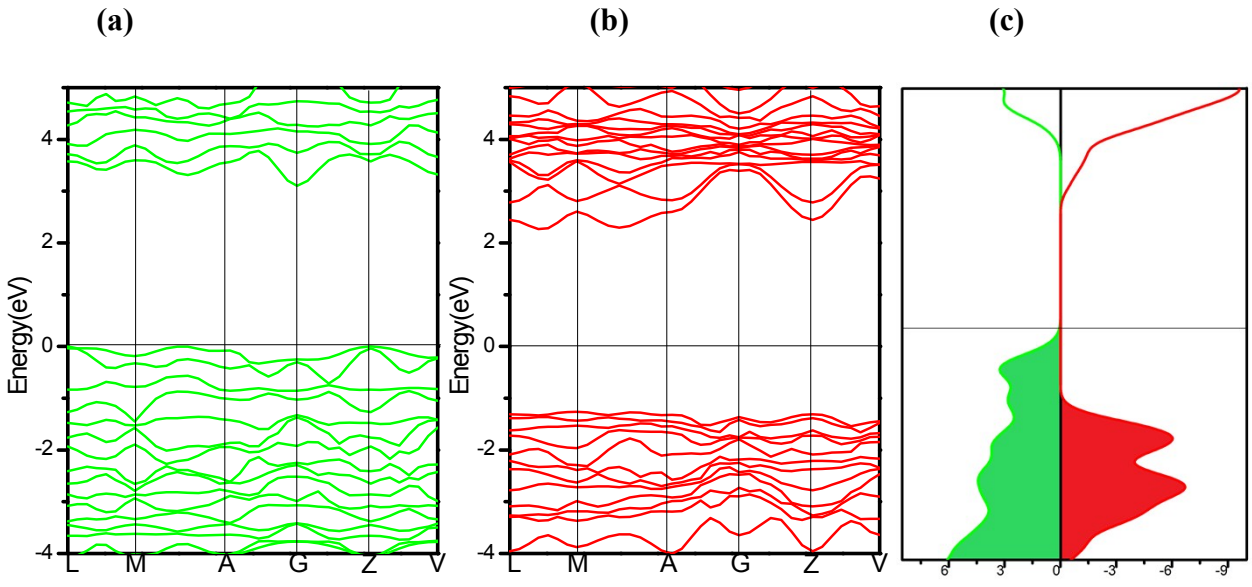

Fig. S13. Band structure of bulk $MnPS_3$ for (a) spin-up (green bands) and (b) spin-down (red bands) configurations. (c) Total density of states (DOS) for both down and up spins. The Fermi level is set as zero energy.

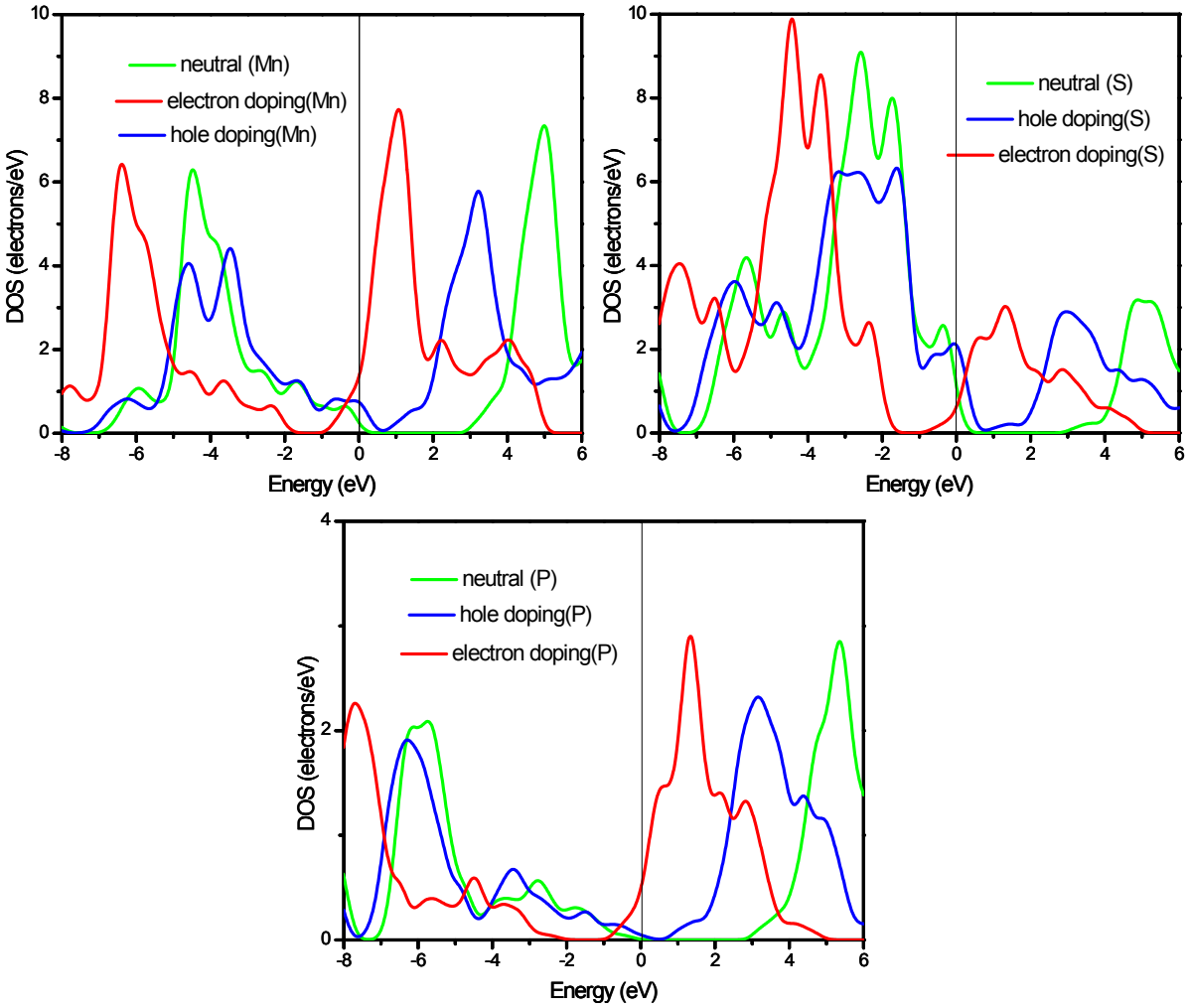

Fig. S14. Atom projected density of states(DOS) of Mn, P and S for $MnPS_3$ with and without electron/hole doping.

Table S5.Geometric parameters for single layer and bilayer $MnPS_3$ using van der Waal correction (D3 function).

Material	Bond length (Å)			Bond angles (°)				Lattice Parameters
	P-S	Mn-S	P-P	Mn-S-Mn	Mn-S-P	S-P-S	S-P-P	
$MnPS_3$ monolayer	2.0463 2.0464	2.6090 2.6080	2.2161	84.25	103.43	113.85 113.84	103.63 103.64	a,b,c= 6.06038, 10.49795, 30.97626 α,β,γ =90, 106.55845,90
$MnPS_3$ (bilayer)	2.0471 2.0500	2.6080 2.6084 2.6073	2.2180	84.67	103.33	114.05 113.85 113.78 113.94	104.64 104.68	a,b,c= 6.060473, 10.49547, 39.47023 α,β,γ =90, 98.93508,90
$MnPS_3$ bulk and neutral	2.0479 2.0509	2.6097 2.6049 2.6060	2.2195	84.16	103.54	114.01 113.97	103.94 104.70	a,b,c= 6.06699, 10.50899, 6.75441 α,β,γ =90, 107.31993, 90

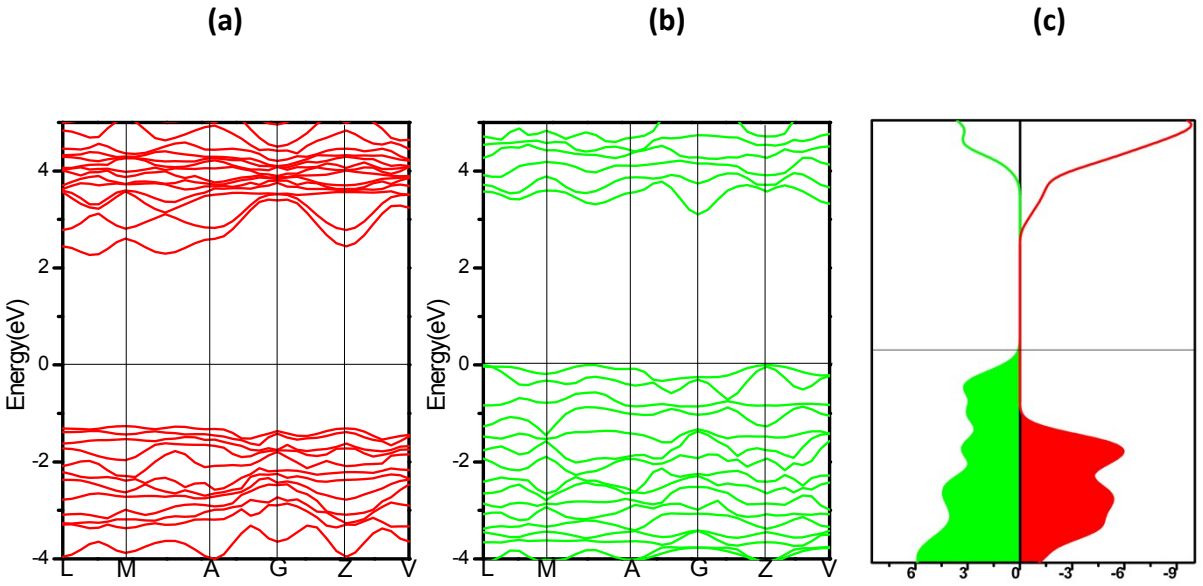

Fig.S15. Band structure calculated with van der Waal's correction for single layer $MnPS_3$ (a) spin-down (red bands) and (b) spin-up (green bands) configurations. (c) Total density of states (DOS) for both down and up spins. The Fermi level is set as zero energy.

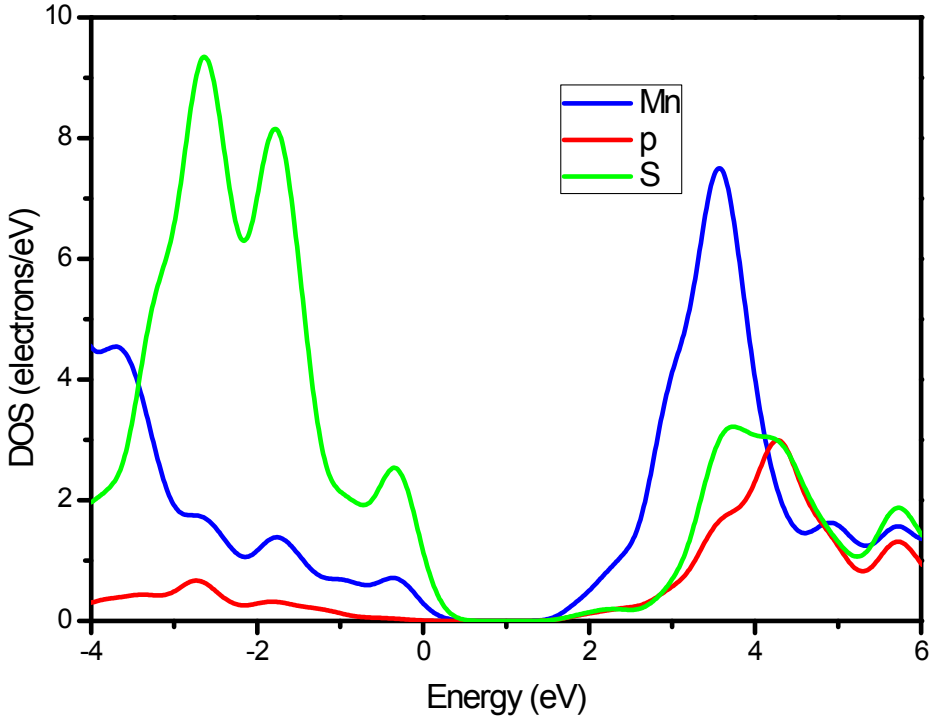

Fig.S16. Atom projected density of states (DOS) for Mn, P and S.

Table: S6. Spin flip gap of bulk, bi-layer and single layer of $MnPS_3$ obtained at the same level of theory (GGA/PBE) with and without van der Waal's correction.

S.No	Material	Δ1(eV)	Δ2(eV)	Δ3(eV)
1	bulk	2.503	1.23	0.77
2	Bi-layer	2.3802	1.2710	0.8102
3	Single layer	2.096	1.29	1.0246
with van der Waal's correction				
4	bulk	2.270	1.26	0.84
5	Bi-layer	2.26	1.3193	0.8747
6	Single layer	2.385	1.26	0.901

References:

[S1]Z. Yin, H. H. Li, H. H. Li, L. Jiang, Y. Shi, Y. Sun, G. Lu, Q. Zhang, X. Chen, and H. Zhang, *ACS Nano*, 2012, **6**, 74.

[S2]O. Lopez-Sanchez, D. Lembke, M. Kayci, A. Radenovic, and A. Kis, Nat. Nanotechnol. 2013, **8**, 497.

[S3]W. Choi, M. Y. Cho, A. Konar, J. H. Lee, G.-B. Cha, S. C. Hong, S. Kim, J. Kim, D. Jena, J. Joo, and S. Kim, *Adv. Mater.* 2012, **24**, 5832.

[S4]N. Perea-Lopez, Z. Lin, N. R. Pradhan, A. Iniguez-Rabago, A. L. Elias, A. McCreary, J. Lou, P. M. Ajayan, H. Terrones, L. Balicas, and M. Terrones, *2D Mater.,* 2014, **1,** 011004.

[S5]D.-S. Tsai, K.-K. Liu, D.-H. Lien, M.-L. Tsai, C.-F. Kang, C.-A. Lin, L.-J. Li, and J.-H. He, *ACS Nano*, 2013, **7**, 3905.

[S6]A. Abderrahmane, P. J. Ko, T. V Thu, S. Ishizawa, T. Takamura, and A. Sandhu, *Nanotechnology*, 2014, **25**, 365202.

[S7]Y.-H. Chang, W. Zhang, Y. Zhu, Y. Han, J. Pu, J.-K. Chang, W.-T. Hsu, J.-K. Huang, C.-L. Hsu, M.-H. Chiu, T. Takenobu, H. Li, C.-I. Wu, W.-H. Chang, A. T. S. Wee and L. -J. Li, *ACS Nano*, 2014, **8**, 8582.

[S8]C. Jung, S. M. Kim, H. Moon, G. Han, J. Kwon, Y. K. Hong, I. Omkaram, Y. Yoon, S. Kim, and J. Park, *Sci. Rep.***,** 2015, **5**, 15313**.**

[S9]L. Yin, X. Zhan, K. Xu, F. Wang, Z. Wang, Y. Huang, Q. Wang, C. Jiang and J. He, *Appl. Phys. Lett.* 2016, **108**, 043503**.**

[S10]N. Perea-Lopez, A. L. Elias, A. Berkdemir, A. Castro-Beltran, H. R. Gutierrez, S. Feng, R. Lv, T. Hayashi, F. Lopez-Urias, S. Ghosh, B. Muchharla, S. Talapatra, H. Terrones and M. Terrones, *Adv. Funct. Mater.,* 2013, **23**, 5511.

[S11]J. D. Yao, Z. Q. Zheng, J. M. Shao and G. W. Yang, *Nanoscale*, 2015, **7,** 14974.

[S12]N. R. Pradhan, J. Ludwig, Z. Lu, D. Rhodes, M. M. Bishop, K. Thirunavukkuarasu, S. A. McGill, D. Smirnov and L. Balicas, *ACSAppl. Mater. Interfaces*, 2015, **7**, 12080,

[S13]J. Chen, B. Liu, Y. Liu, W. Tang, C. T. Nai, L. Li, J. Zheng, L. Gao, Y. Zheng, H. S. Shin, H. Y. Jeong and K. P. Loh, *Adv. Mater.,* 2015, **27**, 6722.

[S14]K. Xu, Z. Wang, F. Wang, Y. Huang, F. Wang, L. Yin, C. Jiang and J. He*, Adv. Mater*., 2015, **27**, 7881.

[S15]S. Yang, S. Tongay, Y. Li, Q. Yue, J.-B. Xia, S.-S. Li, J. Li and S.-H. Wei, *Nanoscale* 2014**,** **6**, 7226.

[S16]F. Liu, S. Zheng, X. He, A. Chaturvedi, J. He, W. L. Chow, T. R. Mion, X. Wang, J. Zhou, Q. Fu, H. J. Fan, B. K. Tay, L. Song, R.-H. He, C. Kloc, P. M. Ajayan and Z. Liu, *Adv. Funct. Mater.* 2016, **26**,1169.

[S17]E. Zhang, Y. Jin, X. Yuan, W. Wang, C. Zhang, L. Tang, S. Liu, P. Zhou, W. Hu and F. Xiu, *Adv. Funct. Mater.,* 2015, **25**, 4076.

[S18] E. Liu, M. Long, J. Zeng, W. Luo, Y. Wang, Y. Pan, W. Zhou, B. Wang, W. Hu, Z. Ni, Y. You, X. Zhang, S. Qin, Y. Shi, K. Watanabe, T. Taniguchi, H. Yuan, H. Y. H. wang, Y. Cui, F. Miao and D. Xing, *Adv. Funct. Mater*. 2016, **26**, 1938.

[S19]S. Yang, Y. Li, X. Wang, N. Huo, J.-B. Xia, S.-S. Li and J. Li, *Nanoscale*, 2014, **6**, 2582.

[S20]P. Hu, Z. Wen, L. Wang, P. Tan and K. Xiao, *ACS Nano*, 2012, **6**, 5988.

[S21]Y. Cao, K. Cai, P. Hu, L. Zhao, T. Yan, W. Luo, X. Zhang, X. Wu, K. Wang and H. Zheng, *Sci. Rep., 2015,* ***5***, 8130.

[S22]F. Liu, H. Shimotani, H. Shang, T. Kanagasekaran, V. Zolyomi, N. Drummond, V. I. Fal'ko and K. Tanigaki, *ACS Nano*, 2014, **8**, 752.

[S23]Z. Wang, M. Safdar, M. Mirza, K. Xu, Q. Wang, Y. Huang, F. Wang, X. Zhan and J. He, *Nanoscale*, 2015, **7**, 7252.

[S24]S. R. Tamalampudi, Y.-Y. Lu, U. R. Kumar, R. Sankar, C.-D. Liao, B. K. Moorthy, C.-H. Cheng, F. C. Chou and Y.-T. *Chen, Nano Lett.,* 2014, **14**, 2800.

[S25]R. B. Jacobs-Gedrim, M. Shanmugam, N. Jain, C. A. Durcan, M. T. Murphy, T. M. Murray, R. J. Matyi, R. L. Moore and B. Yu, *ACSNano* 2014, **8**, 514.

[S26] K. Lai, H. Peng, W. Kundhikanjana, D. T. Schoen, C. Xie, S. Meister, Y. Cui, M. A. Kelly and Z.-X. Shen, *Nano Lett*., 2009, **9**, 1265.

[S27]Y. Huang, H.-X. Deng, K. Xu, Z.-X. Wang, Q.-S. Wang, F.-M. Wang, F. Wang, X.-Y. Zhan, S.-S. Li, J.-W. Luo and J. He, *Nanoscale*, 2015, **7**, 14093.

[S28.] Y. Sun, H. Cheng, S. Gao, Z. Sun, Q. Liu, Q. Liu, F. Lei, T. Yao, J. He, S. Wei, Y. Xie, *Angew. Chemie Int. Ed*., 2012, **51**, 8727.

[S29]R. K. Ulaganathan, Y.-Y. Lu, C.-J. Kuo, S. R. Tamalampudi, R. Sankar, K. M. Boopathi, A. Anand, K. Yadav, R. J. Mathew,C.-R. Liu, F. C. Chou, Y.-T. Chen, *Nanoscale,* 2016, **8**, 2284.

[S30]J. O. Island, M. Buscema, M. Barawi, J. M. Clamagirand, J. R. Ares, C. Sanchez, I. J. Ferrer, G. A. Steele, H. S. J. van der Zant and A. Castellanos-Gomez, *Adv. Opt. Mater.,* 2014 **2**, 641.

[S31]M. Buscema, D. J. Groenendijk, S. I. Blanter, G. A. Steele, H. S. J. van der Zant and A. Castellanos-Gomez, *Nano Lett*., 2014, **14**,3347.

[S32]M. Engel, M. Steiner and P. Avouris, *Nano Lett.,* 2014, **14**, 6414.